Acetic Acid Vapor: 1. Statistical/Quantum Mechanical Models of the Ideal Vapor

Sarah M. Lofgren, Paul R. Mahling, and James B. Togeas*

Division of Science and Mathematics, University of Minnesota, Morris, 600 East 4th Street, Morris, Minnesota, 56267

Received: January 11, 2005; In Final Form: April 20, 2005

Two statistical mechanical/quantum computational models are developed for the ideal acetic acid vapor. One describes the equilibrium of the cis-monomer and the ring dimer and the other the equilibrium of a mixture of oligomers. Ten quantum computational models of the acetic acid ring dimer have been compared in developing these models. The end product of this work is a critical tool for assessing experimental vapor density studies of acetic acid reported in the literature.

1. Introduction

The five most recent experimental vapor density studies of acetic acid vapor have the standard enthalpy of dissociation of the acetic acid dimer ranging from 58 to 69 kJ mol^{-1}. In this paper, statistical mechanical/quantum computational models of the ideal vapor are developed, which are to be used as critical tools to assess the reported results of the experiments. The actual assessment is carried out in a subsequent paper, in which it is argued that the experimental results are consistent with a narrower range of dissociation enthalpies (viz., 65−66 kJ mol^{-1}) at absolute zero. Two models of the ideal vapor are developed in this paper, which will be referred to as *the ring-dimer model* and *the vapor model*. The development of the models requires a large input of empirical information besides that obtained by computation from first principles.

The ring-dimer model is for the dissociation of the ring dimer into two molecules of cis-monomer in the ideal vapor state. There are three components to the model. The first is called the rotation parameter, which depends on the principal moments of inertia of the ring dimer and cis-monomer, and other physical constants. The second component is the vibrational manifolds of the ring dimer and cis-monomer. The third is the dissociation energy, zero-point vibrational energy corrected, of the ring dimer into two molecules of cis-monomer. It is argued in the body of this paper that, with qualifications that are not at all restrictive, the rotation parameter and vibrational manifolds are known and that, as a consequence, the dimer's dissociation energy can be found from the experimental results reported in the literature. For ease of reference, this energy will be called the *empirical dissociation energy* even though it also depends on theoretical quantities. In the subsequent paper, it will be shown that this method leads to the narrower range of enthalpies of dissociation alluded to in the opening paragraph.

To be used successfully in the ring-dimer model, the experimental data must refer to conditions of temperature and pressure under which the vapor is ideal and the only two molecules present in significant quantities are the ring dimer and cis-monomer. The vapor model serves that purpose. It describes the equilibrium of an ideal vapor of 18 oligomers or *n*-mers, $n = 1-4$, as a function of temperature and pressure and shows that at sufficiently low pressure and temperature the requisite conditions are met.

A simple distinction between the two models is that the vapor model describes many equilibria whereas the ring-dimer model describes only one. Another is that the dissociation energy of the ring dimer is found from experimental data in the ring-dimer model, whereas in the vapor model, the dissociation energy of all *n*-mers is found by quantum computation. This raises the question of which level and basis set is best used for the vapor model. Ten different quantum computational models are tested. Of these, the Hartree−Fock (HF) level with the 6-31G(d) basis set gives the best approximation of the empirical dissociation energy. Given this result, it seems natural to use the HF/6-31G(d) method for all of the *n*-mers in the vapor model.

It is seen that the ring-dimer model and the vapor model must be developed in tandem, since the vapor model is needed to determine the conditions under which the ring-dimer model can be applied, and the ring-dimer model is needed to determine which quantum computational method should be used for the vapor model. Ultimately, the validity of the two models depends on their self-consistency and their joint resistance to being proved false.

Section 2 describes the statistical mechanical model of the ideal vapor, including the description of the isomerization of one *n*-mer into another, the methods of quantitatively describing the vapor's composition, and the quantum computational methods employed in modeling individual oligomers in the vapor.

Section 3 describes the vapor and ring-dimer models. It describes the structures and molecular parameters of the 18 oligomers and the composition of the saturated vapor according to the former model. It presents the numerical results of the 10 quantum computational models of the ring dimer and describes the method for choosing which of the 10 is best.

Most of the discussion is deferred to section 4, which includes observations and generalizations about quantum computational methods derived from the ten studies of the ring dimer. The statistical mechanical/quantum computational studies of the oligomers in the vapor reveal simple quantitative "rules of thumb" about their standard enthalpies of isomerization. Literature results are discussed and compared to this work.

Conclusions and summaries are presented in section 5.

* To whom correspondence should be addressed: e-mail <togeasjb@morris.umn.edu>.

10.1021/jp058003r CCC: $30.25
Published on Web 06/01/2005

2. Methods

2.1. Statistical Mechanics. *2.1.1. Dissociation.* For the dissociation of an *n*-mer into monomer, $(HOAc)_n = nHOAc$, the ideal gas thermodynamic equilibrium constant, K_{n1}, is

$$K_{n1} = \frac{P_1^n}{P_n (P^\circ)^{n-1}} = \frac{x_1^n}{x_n}\left(\frac{P}{P^\circ}\right)^{n-1} \tag{1}$$

where x_n is the mole fraction of *n*-mer, P_n is its partial pressure, P is the total pressure, and $P^\circ = 1$ bar. By the methods of statistical mechanics,[1] the equilibrium constant is also

$$K_{n1} = C_n T^{4(n-1)} \frac{\sigma_n}{\sigma_1^n}\left[\frac{(I_{1x}I_{1y}I_{1z})^n}{I_{nx}I_{ny}I_{nz}}\right]^{1/2} \frac{q_{1,\mathrm{vib}}^n}{q_{n,\mathrm{vib}}} \exp\left(-\frac{D_{0,n}}{k_B T}\right) \tag{2a}$$

I_{nx} is the principal moment of inertia of an *n*-mer with respect to the *x*-axis, σ_n its symmetry number, and $q_{n,\mathrm{vib}}$ its vibrational partition function. $D_{0,n}$ is the molecular energy of dissociation of an *n*-mer into *n* moles of monomer, zero-point energy corrected. The *ring* dimer discussed below has C_{2h} symmetry implying that $\sigma_2 = 2$, but the symmetry numbers will be unity for all other species, because they have either C_s or C_1 symmetry. The constant in eq 2a is

$$C_n = \frac{\xi^{n-1}}{n^{3/2}}$$

where

$$\xi = \frac{64\pi^5 {m_1}^{3/2} {k_B}^4}{h^6 P^\circ}$$

The symbols for the Boltzmann and Planck constants are evident; the constant m_1 is the mass of one molecule of acetic acid monomer. Once the principal moments have been found, it is convenient to incorporate them and other constants into a single term and rewrite eq 2a as

$$K_{n1} = F_n T^{4(n-1)} \frac{q_{1,\mathrm{vib}}^n}{q_{n,\mathrm{vib}}} \exp\left(-\frac{D_{0,n}}{k_B T}\right) \tag{2b}$$

The quantity F_n is subsequently referred to as the rotation parameter.

The standard enthalpy and standard entropy of dissociation can be found from the van't Hoff equation and the temperature derivative of the standard Gibbs free energy of dissociation. The results are

$$\Delta H_{n1}^\circ = 4(n-1)RT + nE_{1,\mathrm{vib}} - E_{n,\mathrm{vib}} + N_A D_{0,n} \tag{3a}$$

and

$$\Delta S_{n1}^\circ = R\left[\ln F_n + 4(n-1)(1+\ln T) + \ln\left(\frac{q_{1,\mathrm{vib}}^n}{q_{n,\mathrm{vib}}}\right) + \frac{nE_{1,\mathrm{vib}} - E_{n,\mathrm{vib}}}{RT}\right] \tag{3b}$$

In these equations, $E_{n,\mathrm{vib}}$ is the vibrational *excitation* energy of the *n*-mer (the *zero-point* energy having been incorporated already into the dissociation energy), and N_A is the Avogadro number.

2.1.2. Isomerization. For the isomerization of a reactant *n*-mer into a product *n*-mer, $(HOAc)_n^{(r)} = (HOAc)_n^{(p)}$, the ideal gas thermodynamic equilibrium constant is

$$K_{nn} = \frac{x_{np}}{x_{nr}} \tag{4}$$

where evidently r and p refer, respectively, to reactant and product. By statistical mechanics

$$K_{nn} = \frac{\sigma_r}{\sigma_p}\left[\frac{I_{px}I_{py}I_{pz}}{I_{rx}I_{ry}I_{rz}}\right]^{1/2} \frac{q_{p,\mathrm{vib}}}{q_{r,\mathrm{vib}}} \exp\left(-\frac{D_i}{k_B T}\right) \tag{5a}$$

or

$$K_{nn} = F_{nn} \frac{q_{p,\mathrm{vib}}}{q_{r,\mathrm{vib}}} \exp\left(-\frac{D_i}{k_B T}\right) \tag{5b}$$

in analogy to eqs 2a and 2b. D_i is the molecular energy of isomerization, once again zero-point energy corrected. K_{nn} is a convenient measure of the stability of one isomer with respect to another. In all instances, the reactant will be taken to be the most stable *n*-mer found, which is equivalent to having $K_{nn} < 1$.

The standard enthalpy and entropy of isomerization are found by the same methods as above

$$\Delta H_{nn}^\circ = E_{p,\mathrm{vib}} - E_{r,\mathrm{vib}} + N_A D_i \tag{6a}$$

and

$$\Delta S_{nn}^\circ = R \ln\left(\frac{F_{nn} q_{p,\mathrm{vib}}}{q_{r,\mathrm{vib}}}\right) + \frac{E_{p,\mathrm{vib}} - E_{r,\mathrm{vib}}}{T} \tag{6b}$$

As before, E_{vib} is the vibrational excitation energy.

In eqs 3a and 6a, the difference between excitation energies is small, with the result that the enthalpy changes are approximately given by $\Delta H_{n1}^\circ \approx N_A D_{0,n}$ and $\Delta H_{nn}^\circ \approx N_A D_i$.

2.2. Composition of the Vapor. In the model generated below, 18 oligomers are in simultaneous equilibrium. The composition of the vapor is readily found once the temperature and pressure are specified, and the equilibrium constants have been calculated for that temperature. Since the mole fractions sum to unity, then the mole fraction of cis-monomer, designated x_1, can be found by extracting the root of the quartic equation

$$\sum_{n=1}^{4} A_n x_1^n = 1 \tag{7a}$$

where $A_1 = 1 + K_{11}$, and for $n = 2-4$

$$A_n = \frac{1}{K_{n1}}\left(\frac{P}{P^\circ}\right)^{n-1}\left(1 + \sum_i K_{nn}^{(i)}\right) \tag{7b}$$

In the formula for A_2, for instance, K_{21} is the equilibrium constant for the dissociation of the ring dimer into two moles of cis-monomer, and $K_{22}^{(i)}$ is the equilibrium constant for the isomerization of the ring dimer into the *i*th isomeric dimer. The reference reactions for K_{11}, K_{31}, and K_{41} are described below.

Once the mole fraction of cis-monomer is known, the mole fractions of all other species follow from eqs 1 and 4.

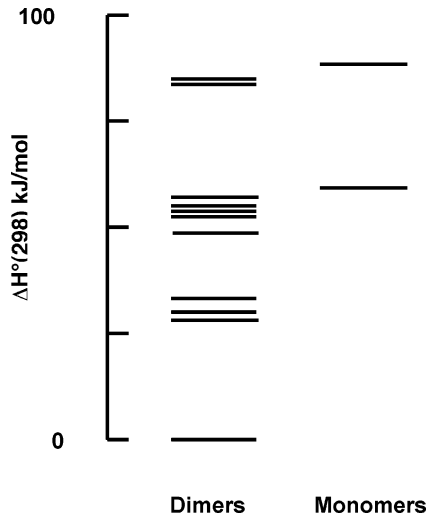

Figure 1. Standard enthalpy of isomerization or dissociation at 298 K.

From here, the apparent molar mass, M, can be found from

$$M = M_1 \sum_n n x_n$$

where $M_1 = 60.05$ g mol^{-1} is the monomer molar mass. The vapor density, d, follows from the ideal gas law.

2.3. Quantum Chemical Calculations. All calculations were done with Spartan '02 for Macintosh[2], version 1.0.4e (Wavefunction, Inc., Irvine, CA). The only semiempirical calculations undertaken were with the parametric method 3 (PM3) technique. Density functional theory (DFT) was applied using the Becke B3LYP exchange-correlation functional. Ab initio calculations were employed at the HF level, which were supplemented by Møller−Plesset second-order perturbation (MP2) methods. The basis sets employed in DFT, HF, and MP2 were 6-31G(d), 6-31G(d,p), and 6-311+G(d,p). Typically calculations were begun with the PM3 method, followed by an intermediate HF/3-21G calculation, and from there to the final model desired.

Vibrational wavenumbers and principal moments of inertia were obtained in PM3, HF, and DFT calculations. Hartree−Fock wavenumbers, as is well-known, are typically too large by about 10%, so the wavenumbers returned in the calculation were multiplied by 0.90. If MP2 calculations were carried out, the "reduced" HF wavenumbers for the basis set were used, since it proved too time-consuming to obtain them directly at the MP2 level.

3. Computational Results

3.1. The Vapor Model. *3.1.1. Introduction.* The vapor was modeled as a mixture of cis- and trans-monomer, ring dimer, eight open dimers, two catemeric dimers, three trimers, and two tetramers. Quantum computations on the *n*-mers were done at the HF/6-31G(d) level and basis set. The rationale for this choice is deferred to section 3.4 below.

3.1.2. Monomers and Dimers. The manifold in Figure 1 portrays their energetics.

In the "dimer ladder," the ring dimer, (**1**), defines the zero of energy. Data for the equilibrium of the ring dimer and two molecules of cis-monomer, (**2**), are given in Table 1 along with data for the most stable trimer and tetramer. The energy of two cis-monomers corresponds to the lower rung in the monomer ladder, whereas the second corresponds to one cis- and one trans-monomer, (**3**). Above the ring dimer is a low-lying set of three dimers, the lowest being the catemeric dimer (**4**), followed by the two open dimers (**5**) and (**6**). The catemers are discussed in section 4. Table 2 gives computed results for isomerization of the most stable *n*-mers, $n = 1-4$, into less stable *n*-mers.

TABLE 1: Dissociation of *n*-Mers into *n* cis-Monomers

n-mer	F_{n1}	ZPVE[a]	$D_{0,n}$	$K_{n1}(298)$	$\Delta H^\circ_{n1}(298)$	$\Delta S^\circ_{n1}(298)$
(**1**) $n = 2$	4.5110	321.99	0.9928	2.010(−3)	58.77	145.5
(**7**) $n = 3$	17.867	482.19	1.2142	1.702	68.30	233.5
(**10**) $n = 4$	310.91	643.63	1.7630	27.82	98.91	359.4

[a] ZPVE is the zero-point vibrational energy. Units of ZPVE and $\Delta H°(298)$ are kilojoules/mole, of $\Delta S°(298)$ joules/mole-K, of $D_{0,n}$ 10^{-19} joules, and of F_{n1} $K^{-4(n-1)}$.

TABLE 2: Isomerization of *n*-Mers[a]

n-mer	F_{nn}	ZPVE	D_i	$K_{nn}(298)$	$\Delta H^\circ_{nn}(298)$	$\Delta S^\circ_{nn}(298)$
(**3**) $n = 1$	1.0083	156.99	0.4791	1.112(−5)	29.25	3.26
(**4**) $n = 2$	2.3801	320.20	0.4394	3.802(−4)	27.69	27.39
(**5**) $n = 2$	2.2285	319.84	0.4716	4.181(−4)	29.88	35.53
(**6**) $n = 2$	2.4492	319.96	0.5236	8.169(−5)	32.77	31.66
(**8**) $n = 3$	1.1258	482.02	0.1053	5.578(−2)	6.42	−2.46
(**9**) $n = 3$	0.9528	482.20	0.0904	2.311(−2)	5.11	−14.19
(**11**) $n = 4$	0.9423	643.87	0.0605	5.349(−1)	3.77	7.46

[a] F_{nn} is dimensionless. Other quantities have the units of their analogues in Table 1. Refer to eqs 5a−b and 6a−b and accompanying text for explanation of symbols.

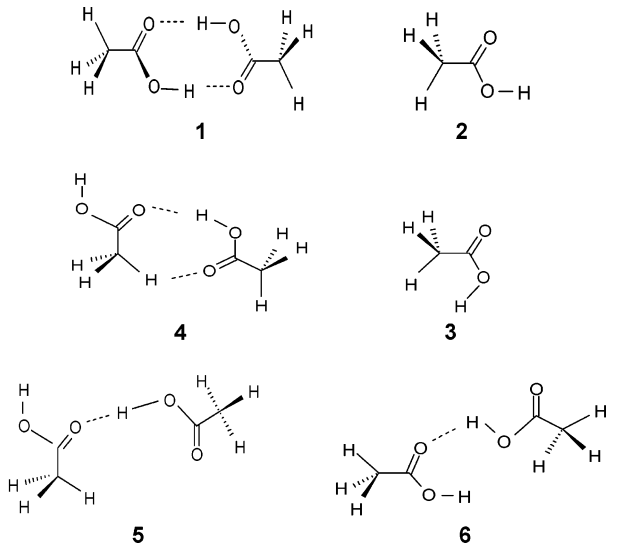

Evidently, the computed results for the three dimers (**4**), (**5**), and (**6**) are so similar that, at this level of approximation, it cannot with confidence be said that one is more stable than the other.

The seven remaining dimers have little effect on the chemistry of the vapor, and thus, their presence can be accounted for in a simplified manner. Instead of seven molecules with their own values of F_{22}, zero-point vibrational energy (ZPVE), and D_i, they are treated as a single molecule with characteristic values of $F_{22} = 2.4065$ and ZPVE = 319.96 kJ/mol, which are the median values for the set of seven, and with seven values of D_i, as though these were excited electronic states. Once again, the isomerization energies are ZPVE corrected. Then, the equilibrium constant for the isomerization of the ring dimer, (**1**), into this hypothetical molecule with

TABLE 3: The Seven High-Energy Dimers

i	1	2	3	4	5	6	7
D_i	0.8010	0.8775	0.8806	0.8814	0.9179	1.355	1.375
ΔH°_{22} (298)	49.27	54.04	54.27	54.21	56.88	83.33	84.77
ΔS°_{22} (298)	28.38	23.93	25.26	17.36	38.93	37.62	47.10

seven electronic states is

$$K_{22}^{(7)} = F_{22}\frac{q_{\mathrm{vib},7}}{q_{\mathrm{vib},ring}}\sum_{i=1}^{7}\exp\left(-\frac{D_i}{k_{\mathrm{B}}T}\right) \qquad (8)$$

Table 3 lists data for the individual seven high-energy dimers. $\Delta H^\circ_{22}(298)$ refers to Figure 1. High-energy dimer $i = 3$ is the trans conformer of the catemeric dimer, and the rest are open dimers. At 298.15 K, $K_{22}^{(7)} = 1.064(-7)$, which, when compared to the equilibrium constants in Table 2, illustrates the exceedingly small, collective contribution of the seven high-energy dimers. Since their effect is so small, their structures are not shown.

3.1.3. Trimers. All three trimers, (**7**)−(**9**), have C_1 symmetry that is nearly C_s. Trimer (**7**), with a ten-membered ring, is the most stable of the three, its parameters being described in Table 1. Turi and Dannenberg[3] proposed a bridged structure for the trimer, but when it was used as a starting point, it evolved into structure (**7**) on geometry optimization. Trimer (**8**) is the catemer. Ritter and Simons[4] proposed a trimer belonging to the C_{3v} point group with twelve atoms (three C, three H, and six O) closing a triply hydrogen-bound ring; the energy minimization that began with that structure led to a distorted version of their proposal, trimer (**9**). An open trimer with its carboxylic acid functionalities in the cis-conformation on energy minimization evolved into the catemeric trimer (**8**). If there are eight open dimers, it would seem there must be more than eight open trimers, but fortunately, the purpose behind developing the vapor model (to have a critical tool for evaluating experimental vapor density studies) does not require the daunting task of delineating all possible *n*-mers.

3.1.4. Tetramers. The tetramer labeled (**10**), which is the more stable of the two, is simply trimer (**7**) with an acetic acid molecule hydrogen-bonded to what had been the free carbonyl group in (**7**). Tetramer (**11**) is the catemer derived from trimer (**8**).

3.2. Composition of the Vapor. The vapor model described above leads to the following predictions about the composition of the vapor. (1) The cis-monomer and the ring dimer will always be the dominant species present. (2) The population of dimers (**4**), (**5**), and (**6**) becomes significant at high temperatures. (3) The mole fractions of trimer and tetramer will be insignificant under any circumstances.

Figure 2 is a semilog plot of the composition of the *saturated* vapor. Since this corresponds to the maximum pressure at which the vapor can exist at each temperature, it also shows the maximum mole fractions of trimer and tetramer at each temperature. The diagram illustrates the dominance of cis-monomer and ring dimer in the oligomer population. The population of the "ten minor dimers" is dominated by dimers (**4**), (**5**), and (**6**). The graph is of course an approximate one, since the high vapor pressures at, say, 400 K will not produce an ideal vapor.

Energy considerations favor the ring dimer. If only energetics were important, then the three dimers (**4**), (**5**), and (**6**) would be the next most commonly encountered species. However, entropy will always favor the monomer, as will low pressure. Thus, the cis-monomer achieves importance due to the interplay of all three factors. In principle, significant amounts of trimer and tetramer could be produced at high pressures, but before that can occur, the vapor phase disappears into the liquid.

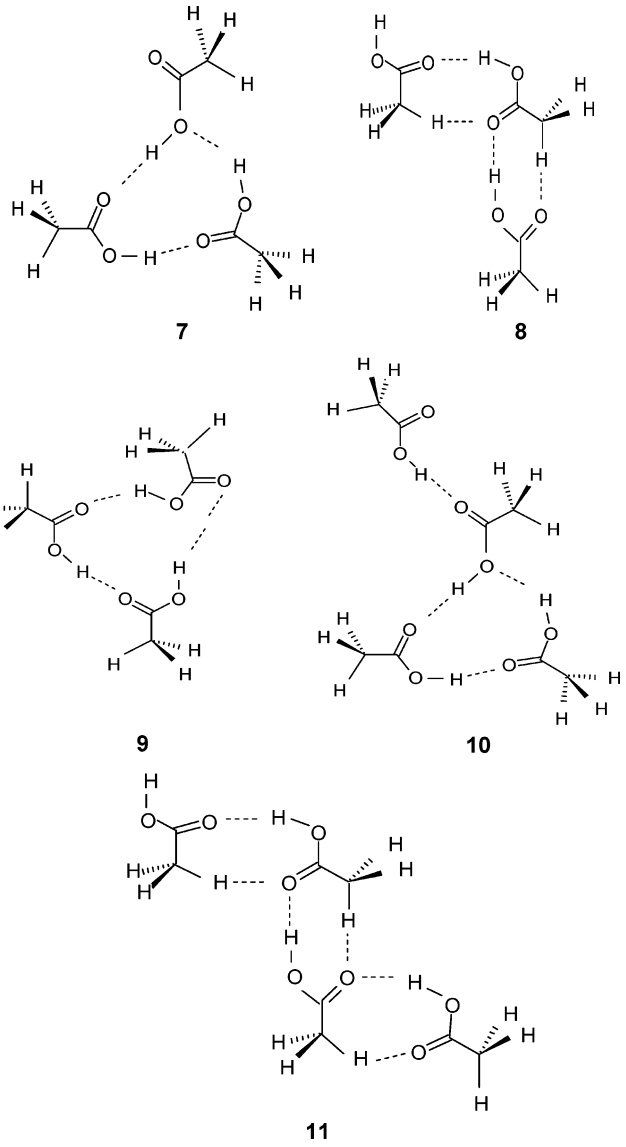

The temperatures in some experimental vapor density studies push into the range 475−500 K and even in a few instances beyond. A typical pressure might be, say, 100 Torr. The vapor model shows that, at 100 Torr and 300 K, the ring dimer accounts for 99.9% of the dimer population, but by 500 K has

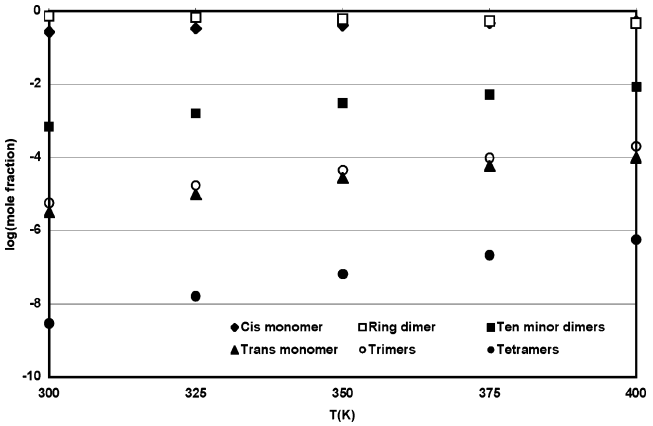

Figure 2. Composition of saturated vapor.

TABLE 4: Quantum Chemical Models of the Ring Dimer[a]

model	F_2	$D_{0,2}$	$K_{21}(298)$	$\Delta H^\circ_{21}(298)$	$\Delta S^\circ_{21}(298)$
PM3	4.7680	0.4603	3.634(+3)	28.26	163.0
HF/6-31G*	4.5110	0.9928	2.010(−3)	58.77	145.5
HF/6-31G**	4.5047	0.9805	3.760(−3)	58.26	149.0
HF/6-311+G**	4.4512	0.8295	1.244(−1)	49.07	147.3
MP2/6-31G*	4.8272	1.2014	1.355(−5)	71.33	146.0
MP2/6-31G**	4.9083	1.2040	1.793(−5)	71.73	149.7
MP2/6-311+G**	4.8871	0.9740	4.770(−3)	57.88	149.7
DFT/6-31G*	4.9213	1.2690	2.066(−5)	76.93	168.4
DFT/6-31G**	5.0052	1.3058	8.354(−6)	79.18	168.3
DFT/6-311+G**	4.8977	0.9920	1.567(−2)	60.08	166.9

[a] Units are the same as in Table 1. G* and G** mean, respectively, G(d) and G(d,p).

fallen under 90%. Experimentalists often calculate the equilibrium constant for ring-dimer dissociation, K_{21}, at a given temperature from the pressure, P, apparent molar mass, M, and monomer molar mass, M_1, from the equation

$$K_{21} = \frac{(2M_1 - M)^2}{M_1(M - M_1)} \frac{P}{P^\circ} \tag{9}$$

However, the vapor model leads to the conclusion that what is actually measured is not K_{21}, but instead (see eq 7b)

$$K_{21}(\text{apparent}) = \frac{K_{21}(\text{actual})}{1 + \sum_k K_{22}^{(k)}} \tag{10}$$

the sum in the denominator being over the minor dimers, that is, over dimers (**4**), (**5**), (**6**), and the "collective" dimer defined by eq 8. At 300 K, the difference between the apparent and actual values is negligible, but at 500 K is about 10%.

3.3. Quantum Computational Models of the Ring Dimer. The results for ten different models are given in Table 4. Their assessment appears in section 3.4.

3.4. The Ring-Dimer Model. The ring-dimer model allows comparison of the results in Table 4 to empirical data. The details of the model are developed below, but the following are the broad-brush principles. Low-pressure empirical data are employed corresponding to the vapor in an ideal gas state, which in turn corresponds to the statistical mechanical model described in section 2.1. Low-temperature empirical data are employed such that there will be few oligomers present other than the cis-monomer and the ring dimer. As a consequence, the cis-monomer/ring dimer equilibrium alone will determine the vapor's density. The equilibrium constant K_{21} is found from the reported pressure, temperature, and density. The three components of the ring-dimer model are (i) the rotation parameter, F_2, (ii) the dissociation energy, $D_{0,2}$, and (iii) the vibrational manifolds for the cis-monomer and the ring dimer. If some plausible choice of F_2 and vibrational manifold can be made, then eq 2b can be solved for a reliable estimate of the molecular dissociation energy, $D_{0,2}$. The best quantum computational model will be the one that best matches the empirically estimated value of $D_{0,2}$.

The differences in the entropies of dissociation in Table 4, especially between the DFT models, on one hand, and the HF and MP2, on the other, are mainly due to differences in vibrational manifolds. Rather than bias the ring-dimer model toward either one of these two sets, the "best" or "optimum" manifolds as described and evaluated by Turi and Dannenberg[5] were chosen. For the monomer, these are the experimental wavenumbers of the normal modes of the cis-monomer and the MP2/6-31G(d) wavenumbers for the ring dimer, which are reported in their paper.

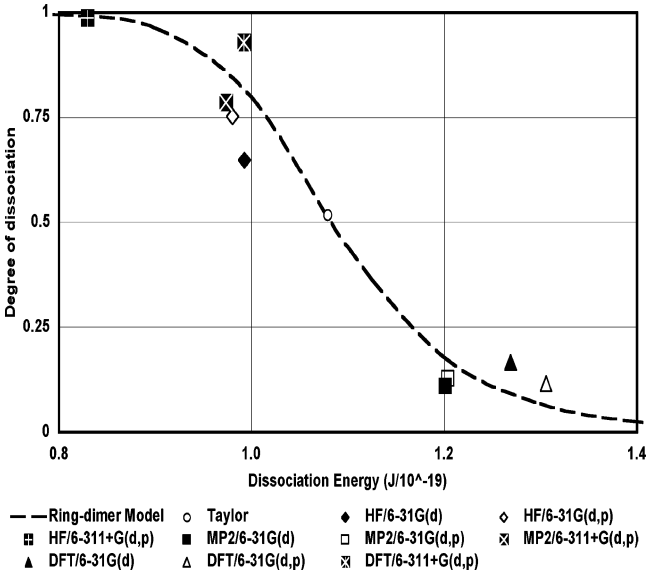

Figure 3. Ring-dimer model and quantum computations compared.

Equations 3a and 3b show that the vibrational manifolds contribute *explicitly* to both the standard enthalpy and entropy of dissociation. For purposes of fitting empirical data to the ring-dimer model, the equations show that F_2 and $D_{0,2}$ can be treated as independent adjustable parameters. The method will be to select a value of the former and calculate the corresponding value for the latter. Table 4 shows that the range of plausible values for the rotation parameter is narrow, and it is shown below that the calculated value of $D_{0,2}$ is insensitive to the choice of F_2 within that narrow range. Determining the dissociation energy for the ring-dimer model ultimately depends on many experimental points, but the complete treatment will be deferred to the paper that is the companion to this one. The fitting is illustrated here for one experimental data point.

Choose a value of $F_2 = 4.5110\ \text{K}^{-4}$, which, from Table 4, is the rotation parameter for the HF/6-31G(d) method. By the ideas elaborated in section 3.2, the data point should correspond to a low temperature, since at high temperatures, the dimer population is contaminated by the minor dimers. A data point from Taylor's paper,[6] $T = 364.2$ K and $P = 37.48$ Torr, seems like a suitable candidate, since the low pressure favors ideal behavior, while the vapor model predicts that the non-ring-dimer population is only 1.7 ppt of the total dimer population, and the trans-monomer is only 100 ppm of the total monomer population. Taylor's data analysis gives the degree of dissociation as $\alpha = 0.5174$, corresponding to $K_{21}(364.2) = 0.0731$, where K_{21} is found from

$$K_{21} = \frac{4\alpha^2}{1 - \alpha^2} \frac{P}{P^\circ} \tag{11}$$

These are the target numbers, represented by the open circle in Figure 3. The units of the abscissa are in 10^{-19} J. By direct calculation from eq 2b, a value[7] of $D_{0,2} = 1.0790 \times 10^{-19}$ J reproduces the values of the equilibrium constant and degree of dissociation given above.

Figure 3 shows that the HF/6-31G(d) method gives the best approximation to the molecular dissociation energy/degree of dissociation given by the ring-dimer model and Taylor's data point. The PM3 method is off-scale to the left. It is thought

that correlated electron models give the best approximations to energies of individual molecules, so it might seem surprising that a Hartree−Fock model with uncorrelated electrons works best here. However, the model is not for one molecule but for three (one dimer and two identical monomers) reacting molecules. Apparently, there is a fortuitous cancellation of the errors associated with noncorrelated models.

Given that the HF/6-31G(d) method gives the best approximation to the empirical dissociation energy, and in the absence of evidence that it should not be used for other oligomers, it seemed natural to choose it for computations on all of the oligomers. The result is also fortunate, since after the PM3 method, which is clearly inadequate to the task at hand, it is the most computationally efficient.

The fact that the rotation parameter for the HF/6-31G(d) method was used in constructing the ring-dimer model by no means biased the analysis in favor of the former. Table 4 shows that the range of rotation parameters is narrow. If the procedure is repeated with, say, $F_2 = 4.900\ \mathrm{K}^{-4}$, the result is $D_{0,2} = 1.0829 \times 10^{-19}$ J. The dissociation energy has changed by only 4 ppt, Figure 3 is essentially the same, and the HF/6-31G(d) model still looks best.

4. Discussion

4.1. Monomers and Dimers. The molecular isomerization energy of cis- to trans-monomer is 4.791(−20) J according to Table 2, which corresponds to an energy difference at 0 K of 28.85 kJ mol^{-1} or 6.896 kcal mol^{-1}, comparable to other values reported in the literature.[8]

X-ray diffraction studies[9] suggest that crystalline acetic acid is a high-molar-mass polymer of the cis-catemeric dimer (**4**). Raman and UV−vis studies[10] suggest that the liquid consists of oligomers—fragments—of this polymer, but no ring dimer. Consistent force field studies[11] provide an explanation for the condensed-phase preference of the catemeric species over the ring dimer, the latter in acetic acid being a vapor-phase species only. Most carboxylic acids do not form chains in the crystalline state.

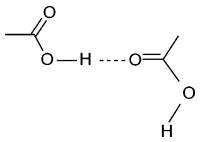

Jentschura and Lippert[12] proposed the above structure for an open dimer and stated that eight planar, open dimers could be generated from this as a starting structure. Although they did not explain their procedure for generating them, their structure provided a convenient point of departure for seeking out the open isomers. Eight structures can be produced by a 180° rotation about the C−O bond in the left-hand moiety, a 180° rotation about the carbonyl in the right-hand moiety, and by choosing cis and trans conformers of the free carboxyl. These eight were starting conformers for variational calculations. Among the eight products, three had C_s symmetry and five C_1, but there does not appear to be a simple correlation between symmetry and stability. Jentschura and Lippert assumed that the eight open dimers would all have about the same energy (viz., the energy required to break a single hydrogen bond), which they took from Moelwyn-Hughes's classic text.[13] At 298 K, this is about 26 kJ mol^{-1}, which would put all eight open isomers just a little below where dimers (**4**), (**5**), and (**6**) appear in Figure 1. Their claim is equivalent to asserting that K_{22} is virtually the same for all of the open conformers, whereas the results of the vapor model calculations, not reported here in their entirety, show that at 298 K K_{22} varies over 9 orders of magnitude.

TABLE 5: Hydrogen-Bond Dissociation and Isomerization Enthalpies[a]

structural unit	$\Delta H°$	unit or isomerization	$\Delta H°$
(**12**)	29−30	(**15**)	34−35
(**13**)	1−2	cis → trans	29
(**14**)	30−32		

[a] Units are kilojoules per mole.

Quantum chemical calculation of all the dimeric structures was also carried out at the DFT/B3LYP/6-31G(d) level and basis set. The resulting manifold does not differ significantly from the pattern in Figure 1.

Structures (**1**), (**4**), (**5**), and (**6**) bear a simple relationship to one another. If the characteristic hydrogen bond of the catemeric dimer (**4**), a methyl-hydrogen-to-carbonyl-oxygen bond, breaks, structure (**5**) is the lowest-energy product available. In the bond-breaking, the symmetry relaxes from C_s to C_1, with one acetic acid moiety rotating out of plane with respect to the other. As a consequence, the energy expense in breaking the bond is offset by an entropy increase. As noted before, the data in Table 2 does not permit a decision as to which is more stable; they appear even closer in stability in the DFT calculation. It appears that breaking one hydrogen bond in the ring dimer would lead directly to open isomer (**6**), with a relaxation from C_{2h} to C_s symmetry; additional relaxation to C_1 could lead to conformer (**5**).

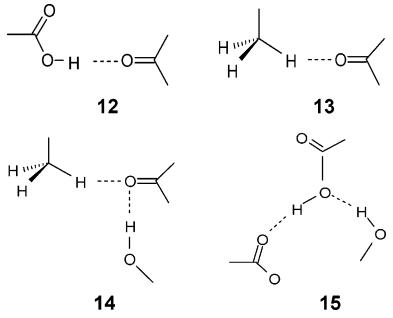

4.2. Hydrogen-Bond Dissociation Enthalpies. The standard enthalpy changes reported in Tables 1 and 2 for 298.15 K can be decomposed approximately into independent contributions from the structural units (**12**)−(**15**) that appear in various *n*-mers. The hydrogen-bond dissociation enthalpies in Table 5 have been deduced from enthalpy changes in those tables for the vapor model. Structural unit (**12**) is the classic hydrogen bond unit. Unit (**13**) is found in all of the catemers and (**14**) in catemers higher than the dimer. Unit (**15**) appears in ring trimer (**7**) and tetramer (**10**). The bond enthalpy for unit (**14**) is obtained by adding those for (**12**) and (**13**). For unit (**15**), add 5 kJ mol^{-1} to that of unit (**12**). To complete the analysis, if an acetic acid moiety is isomerized from cis to trans, as in going from trimer (**7**) to (**9**), add the amount shown in Table 5, which comes from the first row of Table 2.

Here are two examples of how the rules work: (1) Consider the isomerization (**10**) → (**11**). Two units of type (**12**) and one of type (**15**) break, while one each of types (**12**) and (**13**) and two of type (**14**) form. Using the lower values from Table 5 gives

$$\Delta H° \approx -[29 + 1 + 2 \times 30] + 2 \times 29 + 34 = 2\ \mathrm{kJ\ mol^{-1}}$$

From Table 2, $\Delta H° = 3.77$ kJ mol^{-1}. (2) Consider the

TABLE 6: Comparison of Computed Standard Enthalpies of Dissociation of the Ring Dimer[a]

authors	ΔH°_{21}	method	ΔH°_{21} this work	method
T & D	58.6	HF/6-31G(d)	59.57	HF/6-31G(d)
	58.6	HF/6-31G(d,p)	59.05	HF/6-31G(d,p)
	72.8	MP2/6-31G(d)	72.35	MP2/6-31G(d)
N et al.	58.41	HF/6-31G(d,p)	59.05	HF/6-31G(d,p)
	51.50	HF/6-311+G(d,p)	49.95	HF/6-311+G(d,p)
C et al.	66.32	DFT/6-31G(d,p)	84.13	DFT/6-31G(d,p)
	57.6	RI MP2/TZVPP	58.77	MP2/6-311+G(d,p)
F et al.	53.76	LCAO−SCF/STO-3G	58.03	HF/6-31G(d)

[a] Units are kilojoules per mole.

isomerization (**7**) → (**9**). One unit each of types (**12**) and (**15**) breaks, three of type (**12**) form, and a monomer moiety isomerizes from cis to trans. Again, using the lower values in Table 5

$$\Delta H^\circ \approx -3 \times 29 + 29 + 34 + 29 = 5 \text{ kJ mol}^{-1}$$

From Table 2, $\Delta H^\circ = 5.11$ kJ mol^{-1}.

Cautionary notes are appropriate. (i) These rules of thumb roughly work for ring *n*-mers because they have C_s or near-C_s symmetry. Open dimers, by contrast, can depart markedly from this symmetry, with the consequence that conformational effects can contribute to enthalpies of isomerization and the failure of these rules. (ii) The entry for structural unit (**15**) is based on only two examples. (iii) Tables 1, 2, and 5 are based on the vapor model, but the ring-dimer model claims a higher standard enthalpy of dissociation for the ring dimer. (See the companion paper.[20])

4.3. Trimers and Tetramers. Figure 2 illustrates the trends shown in Table 1 that *n*-mers become less stable as *n* increases. The trend seems to be entropy-driven. When an acetic acid moiety in the vapor phase is added to a cyclic $(n-1)$-mer to form a cyclic *n*-mer, new hydrogen bonding leads to an exothermic enthalpy change of about 29−35 kJ mol^{-1} according to Table 5, which is a stabilizing factor. But as *n* increases, so does the standard entropy change. From eq 3b, $\Delta S^\circ_{n1} \approx 4(n-1)R$, which reflects how the equipartition translational and rotational entropies, as well as the stoichiometry, favor *n* mol of monomer over 1 mol of *n*-mer; the same effect appears in eq 2b as $K_{n1} \propto T^{4(n-1)}$. Besides those factors, each added moiety brings in an additional 24 normal modes of vibration, many at low wavenumbers, with the consequence that the vibrational entropy increases rapidly. Hence, the entropy factor overwhelms the enthalpy factor, and *n*-mers greater than the dimer are unimportant in the vapor phase.

4.4. Observations and Generalizations Derived from Table 4 and Figure 3.

1. The semiempirical PM3 model greatly underestimates the dissociation energy, $D_{0,2}$, of the dimer.

2. For a given choice of $D_{0,2}$, the degree of dissociation is estimated in the sequence HF/MP2 < ring-dimer model < DFT. That is, relative to the ring-dimer model's description of how the degree of dissociation varies with dissociation energy, the HF/MP2 models consistently fall below the ring-dimer model's curve and the DFT above it.

3. There is little difference in choosing the 6-31G(d) basis set over 6-31G(d,p) for any level: HF, MP2, or DFT. Thus, the former basis set is preferred, because it is the more economical.

4. Use of the 6-311+G(d,p) basis set over either of the other two leads to a weakening of the hydrogen bond strength at any level: HF, MP2, or DFT.

5. Going from HF to MP2 with any of the three basis sets leads to a stronger hydrogen bond.

4.5. Other Quantum Computational Studies. Turi and Dannenberg[14] carried out semiempirical as well as HF and MP2 calculations with many basis sets on acetic acid monomer and calculations with a subset of these methods and basis sets on the ring and catemeric dimers. Dimer interaction energies were corrected for basis set superposition error (BSSE) as well as ZPVE. They did not treat trimers and tetramers. The enthalpy changes in Table 6 are for absolute zero or $\Delta H^\circ_{21}(0) = N_A D_{0,2}$. For the purposes of comparison, their results for ZPVE but not BSSE corrections were chosen. (The authors state that correcting for both ZPVE and BSSE gives values of $\Delta H^\circ_{21}(0)$ too low relative to experimental results.) The values of $D_{0,2}$ for this work come from Table 4. Their results differ from this work by 0.6−1.6%.

Nakabayashi et al.[15] complemented their Raman studies of liquid acetic acid with HF calculations using the 6-31G(d,p) and 6-311+G(d,p) basis sets on both monomers, on the catemeric dimer, trimer, tetramer, and pentamer, as well as on ring dimer (**1**) and two other high-energy dimers not considered in this paper. They did not carry out BSSE corrections, but their results are ZPVE corrected. Their hydrogen-bonding energies are taken to be values at absolute zero, $\Delta H^\circ_{21}(0)$. Their work and this work differ by 1.1 and 3.1%.

In their study of the acetic acid ring dimer with a variety of theoretical tools, Chocholousová et al.[16] did quantum computations at both the DFT/B3LYP/6-31G(d,p) and RI MP2/TZVPP (RI = resolution of identity) levels, whereas computations in this work have been done at the former but not the latter. The interaction energies, ΔE, reported by these authors refer to differences between potential energy surfaces and have been BSSE but not ZPVE corrected. The result reported for this work is neither ZPVE nor BSSE corrected. Chocholousová et al. do not report the magnitude of their BSSE corrections, but in Turi and Dannenberg's work, the BSSE correction lowers the energy difference by about 10 kJ mol^{-1}. The significance of the comparison remains cloudy. The same is true in the second entry, where the results of two different basis sets are compared.

The paper on thermal conductivity measurements of acetic acid vapor by Frurip et al.[17] includes LCAO-SCF calculations with a minimal STO-3G basis set on the ring dimer. Their results have been ZPVE corrected and reported for 373 K, as has the result of this work. Once again, however, the methods differ, and the comparison is moot.

4.6. The Ring-Dimer Model. In 1978, Chao and Zwolinski[18] reviewed studies on formic and acetic acid vapors. It will be useful to briefly compare their summary with the ring-dimer model. They report principal moments of inertia, which for the cis-monomer had been determined by microwave spectroscopy and for the ring dimer by electron diffraction. These reported results lead to a rotation parameter $F_2 = 4.8143$ K^{-4}, which is

TABLE 7: Ideal Standard Entropies at 298.15 K[a]

source	$S°$ (monomer)	$S°$ (dimer)	$\Delta S°$ (dissociation)
Chao & Zwolinski	283.3	414.3	152.4
ring-dimer model	284.2	412.8	155.5

[a] Units are joules per mole−K.

typical of those in Table 4 and comparable to the value used for the ring-dimer model, $F_2 = 4.5110\ \mathrm{K}^{-4}$.

The moments of inertia and normal modes of vibration can be used to calculate the third-law entropies of ideal vapors by the methods of statistical mechanics. Their results and those of the ring-dimer model are listed in Table 7. The entropy of dissociation for the ring-dimer model also follows from eq 3b. The Berthelot equation of state real-gas correction to the entropy is[19]

$$\frac{27}{32}\frac{RP°}{P_c}\left(\frac{T_c}{T}\right)^3 \approx 1\ \mathrm{J\ mol^{-1}\ K^{-1}}$$

for the critical temperature of 593 K and the critical pressure of 57.81 bar, which implies that the entropies of monomer and dimer are the same at the limit of accuracy of the ideal-gas model.

Thus, the rotational and vibrational parameters of the ring-dimer model and those reported by Chao and Zwolinski are in essential agreement. They will be found to differ, however, in their values of the dissociation energy, or equivalently, of the standard enthalpy of dissociation at absolute zero. After a lengthy critique of vapor density studies reported in the literature using the ring-dimer and vapor models developed here, it is argued in the companion paper that $\Delta H°_{21}(0) \approx 65-66$ kJ mol^{-1}.

5. Summary and Conclusions

1. Ten quantum computational/statistical mechanical models of the ring dimer were developed.

2. A ring-dimer model was developed. Its rotational parameter was derived from the quantum mechanical/statistical calculations. Its vibrational component was taken from a recent critique of spectroscopic measurements and theoretical vibrational studies. The dissociation energy was calculated from pressure, temperature, and density measurements on the ideal vapor.

3. The ring-dimer model picks out the HF/6-31G(d) method as the method of choice for the vapor model, because the HF/6-31G(d) method gives the best estimate of the empirical dissociation energy. The HF/6-31G(d) method is also computationally efficient.

4. The vapor model was used to estimate the composition of a vapor containing 18 *n*-mers, $n = 1-4$. At low pressure and temperature, the cis-monomer and the ring dimer are the only oligomers present in significant quantities. At high temperatures, open dimers compose as much as 10% of the dimer population. Trimer and tetramer populations are always low.

5. The ring-dimer and vapor models can be used to critique experimental vapor studies of acetic acid, which is the subject of the subsequent paper.

Acknowledgment. The authors are grateful to Professor Mike Korth and to the chemistry discipline of the University of Minnesota, Morris, for computing facilities and to Ms. Sandy Kill of Briggs Library for meeting literature requests. J.B.T. is grateful to the Regents of the University of Minnesota for a sabbatical during which this work was completed.

References and Notes

(1) McQuarrie, D. A. *Statistical Mechanics*; Harper Collins: New York, 1976; Chapters 6 and 8.

(2) Kong, J.; White, C. A.; Krylov, A. I.; Sherrill, C. D.; Adamson, R. D.; Furlani, T. R.; Lee, M. S.; Lee, A. M.; Gwaltney, S. R.; Adams, T. R.; Ochsenfeld, C.; Gilbert, A. T. B.; Kedziora, G. S.; Rassolov, V. A.; Maurice, D. R.; Nair, N.; Shao, Y.; Besley, N. A.; Maslen, P. E.; Dombroski, J. P.; Daschel, H.; Zhang, W.; Korambath, P. P.; Baker, J.; Byrd, E. F. C.; Van Voorhis, T.; Oumi, M.; Hirata, S.; Hsu, C.-P.; Ishikawa, N.; Florian, J.; Warshel, A.; Johnson, B. G.; Gill, P. M. W.; Head-Gordon, M.; Pople, J. A. *J. Comput. Chem.* **2000**, *21*, 1532.

(3) Turi, L.; Dannenberg, J. J. *J. Phys. Chem.* **1993**, *97*, 12197.

(4) Ritter, H. L.; Simons, D. H. *J. Am. Chem. Soc.* **1945**, *67*, 757.

(5) See ref 3.

(6) Taylor, M. D. *J. Am. Chem. Soc.* **1951**, *73*, 315.

(7) Five significant digits are carried in values of the molecular dissociation energy to control round-off error in subsequent calculations, but only three significant digits are reported in the final results.

(8) Two recent results are 29.3 kJ mol^{-1} by Nakabayashi et al. (ref 10) at the HF/6-31++G** level and basis set and 25.5 kJ mol^{-1} by Turi and Dannenberg (ref 3) for an MP2/6-311G++(d,p) calculation. The former is for absolute zero and the latter for 298 K. The latter pair of authors provide an extensive table of isomerization energies computed at different levels with different basis sets.

(9) Leiserowitz, L. *Acta Crystallogr.* **1976**, *B32*, 775.

(10) Nakabayashi, T.; Kosugi, K.; Nishi, N. *J. Phys. Chem. A* **1999**, *103*, 8595.

(11) Hagler, A. T.; Dauber, P.; Lifson, S. *J. Am. Chem. Soc.* **1979**, *101*, 5131.

(12) Jentschura, U.; Lippert, E. *Z. Phys. Chem. (Muenchen, Ger.)* **1972**, *77*, 64.

(13) Moelwyn-Hughes, E. A. *Physical Chemistry*, 2nd revised ed.; Pergamon: Oxford, 1964; Chapter 20.

(14) See ref 3.

(15) See ref 10.

(16) Chocholousová, J.; Vacek, J.; Hozba, P. *J. Phys. Chem. A* **2003**, *107*, 3086.

(17) Frurip, D. J.; Curtiss, L. A.; Blander, M. *J. Am. Chem. Soc.* **1980**, *102*, 2610.

(18) Chao, J.; Zwolinski, B. J. *J. Phys. Chem. Data* **1978**, *7*, 363.

(19) Klotz, I. M. *Chemical Thermodynamics*; Prentice Hall: Englewood Cliffs, NJ, 1950; Chapter 10.IV.

(20) Togeas, J. B. *J. Phys. Chem. A* **2005**, *109*, 5438